Letter to the Editor

Synthesis of TiO_2 Nanospikes for Dual Antibacterial Activity*

LI Ze Ping[1,2,&], CHEN Zhi Yuan[3,&], YANG Ming Yan[4], and YI Wei Song[5,#]

Bacterial infections on medical and public surfaces have caused considerable harm to human life and have gained widespread attention. Various surface coating strategies, including the use of antibiotics, metal ions, quaternary ammonium salts, peptides, and carbon-based nanomaterials[1-4], have been developed to improve their antibacterial properties. However, their widespread use may lead to increased bacterial resistance and super bacterial growth, thereby limiting their long-term durability and safety. Drawing inspiration from nature, in which the physical and mechanical properties of dragonfly wings, wall tiger skin, and shark skin have been demonstrated, researchers have developed various artificial nanostructured surfaces[5-7]. This method involves the application of physical forces to nanostructured surfaces to penetrate and destroy bacterial cell walls, delivering antibacterial effects with benefits such as durability, broad-spectrum coverage, heat resistance, low potential for drug resistance, and complete sterilization[8]. Compared to chemical methods, this new physicomechanical approach is safer and more sustainable and has garnered substantial interest recently. However, the antibacterial performance may vary, and different bacterial strains exhibit diverse behaviors on the surface of nanostructures based on their cell wall characteristics, morphology, and mobility[9]. Multi-mechanical antibacterial methods that act synergistically are usually superior to single-mode approaches. Nanostructured TiO_2 has received increasing attention because of its nanoscale effects, biocompatibility, bioactivity, stability, and versatile fabrication techniques.

This study aimed to synthesize TiO_2 with ordered nanospikes through a hydrothermal method, which is a reliable, environmentally friendly, and cost-effective technique for controlling material morphology. The synthesized structure was characterized using field emission scanning electron microscopy (FESEM), X-ray photoelectron spectroscopy (XPS), X-ray diffraction (XRD), and Raman spectroscopy. The TiO_2 nanospikes' ability to generate superoxide anions ($\cdot O_2^-$) and hydroxyl radicals (·OH) under ultraviolet (UV) irradiation was assessed using 1,3-diphenylisobenzofuran (DPBF) and methyl violet optical density measurements. Antibacterial activity was determined by analyzing changes in the colony forming unit (CFU) count and their statistical significance (*P* value). Based on these results, an experimental discussion was conducted to propose an antibacterial mechanism.

Nanospike-structured TiO_2 arrays were synthesized through the hydrothermal reaction of Ti foil in a NaOH solution, followed by ion exchange in a 1 mol/L HCl solution and air annealing, as shown in Supplementary Figure S1, available in www.besjournal.com. After the Ti foil was pre-cleaned and polished, the hydrothermal synthesis was performed at a low temperature of 220 °C for 4–48 h in a sealed autoclave in a muffle furnace. H^+ was then substituted for Na^+ by immersion in a 1 mol/L HCl solution for 15 min, producing $H_2Ti_2O_5 \cdot H_2O$ nanostructures. The final step involved calcining the $H_2Ti_2O_5 \cdot H_2O$ specimens at 650 °C for 1 h in a muffle furnace.

The microstructures of TiO_2 nanospikes samples were examined using FESEM, XPS, Raman spectrometer, and XRD. The surface hydrophilicities of the Ti and TiO_2 nanostructures were measured using a contact-angle instrument (Raméhart, USA) *via* the sessile drop method. Reactive oxygen species

doi: 10.3967/bes2023.124

*This work was supported by the Natural Science Foundation of Hubei Province, China [Grant No. 2021CFB418]; and the National Scientific Research Project Cultivation Program of Hubei University of Science and Technology [2023-25GP01].

1. School of Electronic and Information Engineering, Hubei University of Science and Technology, Xianning 437100, Hubei, China; 2. Key Laboratory of Optoelectronic Information and Intelligent Control, Hubei University of Science and Technology, Xianning 437100, Hubei, China; 3. School of Nuclear Technology and Chemistry & Biology, Hubei University of Science and Technology, Xianning 437100, Hubei, China; 4. Department of Rehabilitation, Xianning Hospital of Traditional Chinese Medicine, Xianning 437100, Hubei, China; 5. College of Science, Huazhong Agricultural University, Wuhan 430070, Hubei, China

(ROS) were determined using DPBF, methyl violet, and methylene blue (MB) dyes. The potential antibacterial efficacy of the samples was examined against *E. coli* (gram-negative) and *S. aureus* (gram-positive) as the test microorganisms.

SEM images revealed a mean diameter of approximately 50 nm for the TiO_2 nanospikes, as shown in Supplementary Figure S2A (available in www.besjournal.com). The uniform diameter along the radial direction of each nanospike suggests that the nanospikes grow upward radially at a rapid pace compared with the lateral direction. The length of the nanowires increased proportionally with hydrothermal growth time, whereas the diameter remained nearly constant, as shown in Supplementary Figure S2A and S2C. Overly extended nanowires tended to curve and unite at the end, resulting in the formation of the morphology shown in Supplementary Figure S2B and S2C, caused by the capillary force during the drying process.

The spectra consisted of O, Ti, and C elements, with carbon potentially originating from the XPS instrument itself, used as a standard signal source. Additionally, high-resolution Ti 2p XPS spectra displayed the oxidation state of Ti^{4+} on the TiO_2 surface, as evidenced by binding energies of 463.94 eV and 458.24 eV for the Ti $2p_{1/2}$ and Ti $2p_{3/2}$ peaks, respectively, which differ by 5.70 eV. Finally, the oxygen ions in TiO_2 were identified *via* high-resolution 1s XPS spectra with a peak at 529.59 eV (Supplementary Figure S3A, available in www.besjournal.com).

No impurity peaks were detected except for Ti peaks (JCPDS card No. 01-1197) originating from the Ti foil (Supplementary Figure S3B). The XRD patterns of the TiO_2 anatase phase and rutile phase closely resemble previously reported patterns[10]. The structures of the TiO_2 nanospikes were analyzed using Raman spectroscopy, which is more sensitive to nanostructures than XRD. Raman peaks of TiO_2 anatase are observed at 144 cm^{-1}, 399 cm^{-1}, 513 cm^{-1}, and 628 cm^{-1}, respectively, corresponding to Eg, B_1g, A_1g, and Eg, as shown in Supplementary Figure S3C. These peaks were consistent with typical Raman features of the anatase phase[10]. The hydrothermal reaction converted a Ti surface with a water contact angle of over 68° into a TiO_2 nanostructured surface with a water contact angle of less than 10°. This transformation indicates improved Ti hydrophilicity owing to the TiO_2 nanostructure, as shown in Supplementary Figure S3D.

DPBF is a fluorescent probe that indicates singlet oxygen with high specificity for $\cdot O_2^-$. The reaction of DPBF with $\cdot O_2^-$ can reduce the absorption intensity to approximately 420 nm. The electrophilic addition reaction of the -c=c- group with a high electron cloud density in methyl violet occurs with ·OH, and the reaction of methyl violet with ·OH decreases the absorption intensity at approximately 580 nm. The amounts of $\cdot O_2^-$ and ·OH generated from the TiO_2 nanospikes under UV irradiation were determined by measuring the change in the optical density of DPBF and methyl violet. As depicted in Figure 1A–B, the sample absorption peak intensity decreased with increasing radiation time, indicating that the TiO_2 nanospikes were excited by UV irradiation to produce $\cdot O_2^-$ and ·OH. The nanostructure of the TiO_2 nanospikes increases the effective surface area for UV absorption and photocatalysis, thereby increasing ROS generation, resulting in the degradation of detection reagents and reduced absorption intensity.

Planar Ti without light irradiation (denoted as sample S1) lacked both physical and photocatalytic antibacterial activity, whereas TiO_2 nanospikes without light irradiation (sample S2) exhibited only physical antibacterial activity through their nanostructure. TiO_2 nanospikes under UV-light irradiation (sample S4) demonstrated both physical and photocatalytic antibacterial activities by producing ROS. Planar Ti under light irradiation (denoted as sample S3) was used to analyze the effect of UV light alone. For the non-UV control, samples were cultured in the dark.

The photostability from ROS generation of TiO_2 nanospikes was quantified using the MB dye under UV illumination, as shown in Figure 1C. ROS produced by TiO_2 bleach the MB dye. When the reaction time was increased by 2 h, samples 2 and 3 maintained relatively high and stable degradation rates for MB, and the MB degradation rate of sample 4 was significantly higher than that of sample 3.

The antibacterial activity against *E. coli* is shown in Figure 2A. The CFU count of S2 was significantly lower than that of planar S1, indicating that S2 possesses intrinsic antibacterial activity. Similarly, the CFU count of S3 showed a more significant decrease because of its physicomechanical and photocatalytic antibacterial activities. Although the CFU count of S1 also decreased slightly, this was likely due to the drying of bacterial droplets and the lack of an antibacterial effect of the Ti material. Notably, the CFU count of S2 decreased slowly at first and then rapidly, suggesting the gradual physical penetration of the cell membrane by the

nanostructure, resulting in concentrated bacterial death at a later stage. The decrease in the CFU count of S3 indicates that UV rays have antibacterial activity. In contrast, the CFU count of S4 decreased quickly at the beginning and then slowed, possibly because of the reduction in active sites on the surface of the nanostructures caused by the adsorption of the reactants and products. These differences in statistical significance (*P*-value) between the different samples were mostly consistent with the observed antibacterial activity. Moreover, the excellent antibacterial performance was attributed to the dual effect of the physicomechanical and photocatalytic antibacterial activities, as described in the following dual antibacterial mechanism. However, Figure 2B shows that the TiO_2 nanospikes have better antibacterial performance against gram-positive bacteria than *E. coli*. This discrepancy could be attributed to variations in the cell wall structure and ROS levels, in addition to the protective role of the outer envelope of gram-negative bacteria.

The proposed antibacterial mechanism based on the experimental results and the discussion presented above is shown in Figure 3. Photogenerated electrons react with the surrounding oxygen to generate ROS, which react with the cell membrane or directly enter the bacteria, leading to the destruction of the bacterial cell membrane (Figure 3A). When the bacterial membrane attempts to contact and colonize the surface of the nanostructure, the tension produced by the nanostructures can generate mechanical stress on the bacterial membrane. This stress may result in the irreversible deformation, stretching, or rupture of the bacterial membrane, ultimately leading to bacterial death (Figure 3B). The resulting damage to bacterial membranes, proteins, and DNA ultimately contributes to bacterial death, as shown in the inset of Figure 3B. The nanospike-structured TiO_2 under UV irradiation enhances the antibacterial effect through the dual effects of physical rupture and ROS production.

In conclusion, the TiO_2 nanospikes synthesized via hydrothermal methods exhibited excellent dual antibacterial activity. Morphological characterization

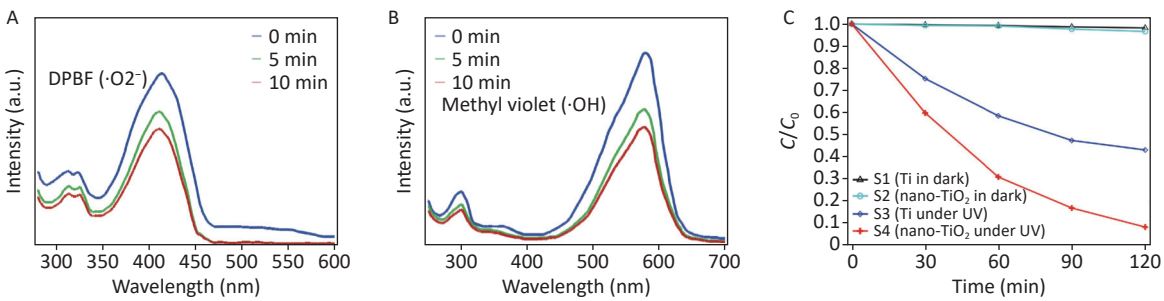

Figure 1. Detection of ROS on TiO_2 nanospikes by measuring the optical density changes of DPBF and methyl violet after UV irradiation for 0–10 min. (A) detection of $\cdot O_2^-$ from the decay of DPBF; (B) detection of ·OH from the decay of methyl violet; (C) MB dye degradation of different surfaces (C is the concentration observed at t min, and C_o is the initial concentration of the dye).

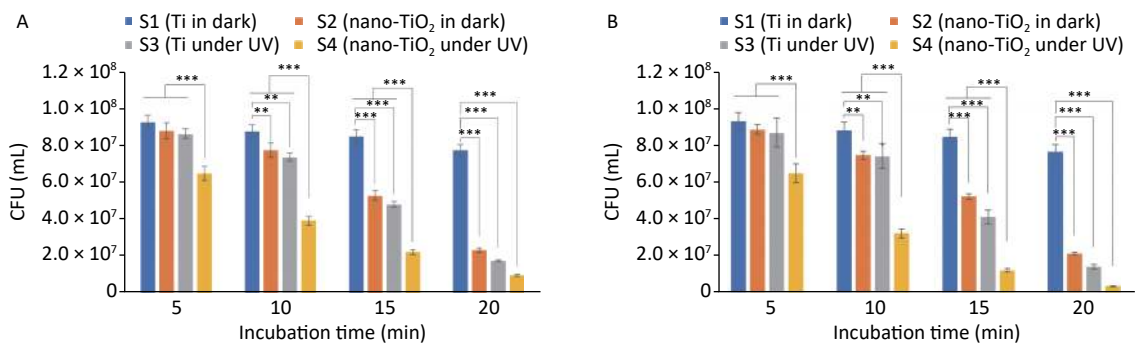

Figure 2. Validation of antibacterial activity in killing (A) *E. coli* and (B) *S. aureus* (Data were presented as mean ± standard deviation. $^{*}P < 0.05$, $^{**}P < 0.01$ and $^{***}P < 0.001$ were considered significant, highly significant, and extremely significant, respectively).

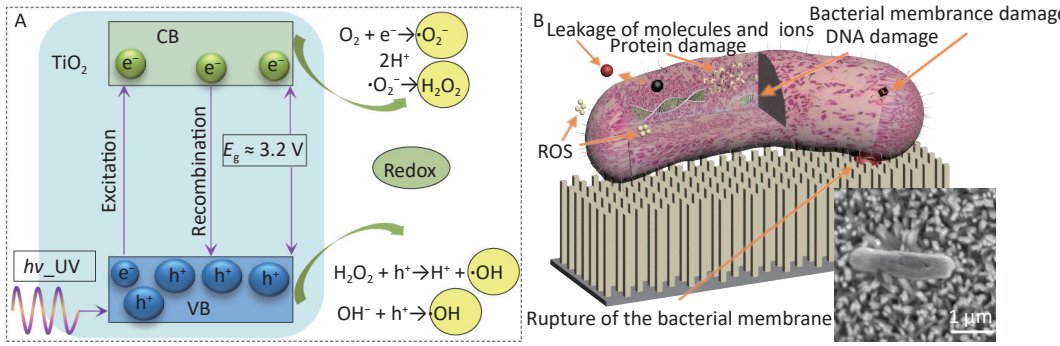

Figure 3. A schematic representation of the mechanism of TiO_2 photocatalysts. (A) photocatalytic mechanism; (B) antibacterial mechanism of nanospike-structured TiO_2, the inset is SEM image of dead *E. coli* bacteria in S2.

and structural investigation revealed that the synthesized TiO_2 nanospikes consisted of anatase/rutile mixed phases with a mean diameter of approximately 50 nm. The amount of ROS generated by $\cdot O_2^-$ and ·OH increased because of the nanostructure of TiO_2, which increased the effective surface area for UV irradiation absorption and photocatalysis, leading to the degradation of detection reagents and a reduction in absorption intensity. The photostability from ROS generation in TiO_2 nanospikes was quantified using MB dye. The changes in the CFU count and statistical significance (*P* value) in the antibacterial activity experiments indicated that the nanostructures significantly improved the antibacterial performance, displaying an extremely significant antibacterial effect owing to the dual antibacterial activity. Finally, based on the experimental results and discussion, an antibacterial mechanism is proposed. The physicomechanical and photocatalytic antibacterial activities of nanostructured TiO_2 materials attribute to their dual antibacterial roles. These results reveal an excellent dual antibacterial approach with great potential in related fields.

[&]These authors contributed equally to this work.

[#]Correspondence should be addressed to YI Wei Song, Professor, E-mail: weisong_yi@mail.hzau.edu.cn

Biographical notes of the first authors: LI Ze Ping, male, born in 1979, Associate Professor, Doctor of Biomedical engineering; CHEN Zhi Yuan, male, born in 1972, Professor, Doctor of Biomedical engineering.

Received: May 6, 2023;
Accepted: July 5, 2023

REFERENCES

1. Wei Q, Liu SX, Huang X, et al. Immunologically effective biomaterials-enhanced vaccines against infection of pathogenic microorganisms. Biosaf Health, 2023; 5, 45−61.
2. Liu C, Guo YQ, Wei XJ, et al. An outstanding antichlorine and antibacterial membrane with Quaternary ammonium salts of alkenes via in situ polymerization for textile wastewater treatment. Chem Eng J, 2020; 384, 123306.
3. Engelberg Y, Landau M. The human LL-37(17-29) antimicrobial peptide reveals a functional supramolecular structure. Nat Commun, 2020; 11, 3894.
4. Linklater DP, Ivanova EP. Nanostructured antibacterial surfaces-what can be achieved? Nano Today, 2022; 43, 101404.
5. Karges J. Combination of chemistry and material science to overcome health problems. Biosaf Health, 2022; 4, 64−5.
6. Wei DX, Zhang XW. Biosynthesis, bioactivity, biotoxicity and applications of antimicrobial peptides for human health. Biosaf Health, 2022; 4, 118−34.
7. Wang XK, Zhang MR, Zhu TT, et al. Flourishing antibacterial strategies for osteomyelitis therapy. Adv Sci, 2023; 10, 2206154.
8. Li SQ, Dong SJ, Xu WG, et al. Antibacterial hydrogels. Adv Sci, 2018; 5, 1700527.
9. Ding JX, Xiao HH, Chen XS. Advanced biosafety materials for prevention and theranostics of biosafety issues. Biosaf Health, 2022; 4, 59−60.
10. Lee CH, Rhee SW, Choi HW. Preparation of TiO_2 nanotube/nanoparticle composite particles and their applications in dye-sensitized solar cells. Nanoscale Res Lett, 2012; 7, 48.